Emerging Spatio-temporal Hot Spot Analysis of Beijing Subsidence Trend Detection Based on PS-InSAR

Wei Zhang[1,2], Tao Zhang[1]*, Zhengbo Fu[1], Ping Ai[1], Guoqing Yao[2], Jianwei Qi[1]

[1] Land Satellite Remote Sensing Application Center, MNR. Beijing 100048, China
[2] China University of Geosciences, Beijing 100083

KEY WORDS: Beijing Subsidence, PS-InSAR, Emerging Hot Spots, Trend Analysis, Sentinel-1

ABSTRACT:

Scholars have done a lot of research on urban settlement, but it is difficult to give consideration to the temporal and spatial attributes of settlement at the same time in its display and analysis. Most of them focused on the analysis of regional settlement, single point settlement curve and settlement rate map at a certain time, but few combined time and space for collaborative analysis. Therefore, in this paper, 32 scenes Sentinel-1B SAR data are used to obtain settlement data of Beijing via PS-InSAR method. Secondly, combined with the temporal and spatial attributes of settlement results, the subsidence law revealed by using spatio-temporal cube slicing and attribute filtering. Finally, subsidence development trend and the detection of abnormal subsidence are explored by emerging hot spots (ESH) analysis. The experimental results show that the settlement funnel center in Beijing is mainly concentrated near the junction of Chaoyang district and Tongzhou district. The settlement range tends to expand. There are several local continuous subsidence areas in the settlement oscillating area. Spatio-temporal analysis makes the development trend of urban settlement more intuitive. Emerging hotspot analysis combined with Getis-Ord Gi* statistics and Mann-Kendall trend test could more effectively analyze the settlement trend of the study area and detect new potential settlement centers, so that to provide auxiliary decision-making for urban safety early warning and city development.

1. Introduction

Land subsidence is a geological phenomenon formed under the combined action of natural and human activities. It develops slowly, has a wide range of influence, has complex causes and is difficult to recover. Among them, urban subsidence is closely related to human life and is an important factor restricting the sustainable development of cities. China 's Yangtze River Delta and North China Plain are highly urbanized areas, and they are also high incidence areas of land subsidence disasters(Yang et al., 2015). In recent years, these cities have continued to expand spatially, and ground subsidence is further intensifying as a result of urban construction(Cigna and Tapete, 2022), underground space and transportation construction, and groundwater extraction. Precision level measurement is the traditional means of urban settlement monitoring, although this method is highly accurate, but the observation period is long, and it is impossible to realize continuous, real-time monitoring. With Ferretti's(Ferretti et al., 2001) proposal of Permanent Scatterer Interferometry PS-InSAR (Persistent Scatterer InSAR), this method overcomes the effect of atmospheric delay factor in DInSAR technique by identifying and decoding long time series of PS points, giving full play to the advantages of remote sensing with large range, high accuracy, and high spatial-temporal resolution(Crosetto et al., 2016), and it is the most widely used and matured method in the field of interferometric radar urban subsidence monitoring.

At present, the analysis and prediction of settlement results is an important work of urban settlement monitoring, and most of the settlement analysis is based on the settlement rate graph, single-point settlement curve graph, and cumulative settlement analysis, which weakens the temporal and spatial attributes of

the settlement data, does not explore the temporal and spatial aggregation of the settlement and the development of the trend of the law, and is insufficient to excavate the information implied by the settlement data. Although there is literature(He et al., 2022) on the use of space-time analysis methods for settlement results, only the Principal component analysis (PCA) method is used, and time is not used as a new dimension for joint analysis.. Since subsidence has strong spatial correlation and is also a process of spatio-temporal dynamic change(Foroughnia et al., 2019), whose pattern fluctuates with changes in seasonal precipitation and drought, groundwater pumping patterns, regional geological differences, etc. This paper takes the PSInSAR subsidence results of Beijing city as the input analytical data source through geographic spatio-temporal analysis method, and selects 290,000 PS points and 32 time scales, and adopts geographic information data ESH analysis to extract more spatio-temporal correlation information on subsidence, such as aggregated temporal and spatial location of subsidence, pattern of development of subsidence, and detection of regional trend of subsidence, which provides a better auxiliary decision-making for the early warning of urban safety and development.

2. Method

2.1 The Algorithm Flow

In this paper, the time series deformation analysis of permanent scatterers is carried out based on 32 scenes of Sentinel-1B data. Based on the settlement results, a space-time cube is established, and then EHS space-time analysis method is used to detect the settlement trend. The main algorithm flow is shown in Figure 1. It is mainly divided into two parts. The first part is the

---

[1] Wei Zhang, Email: dave6806@163.com

* Tao Zhang, Email: zhangtaosas@qq.com

deformation monitoring process based on PS-InSAR. The second part is the spatio-temporal cube analysis and knowledge mining based on the obtained deformation results. The specific contents correspond to the contents of sections 2.2 and 2.3 respectively.

2.2 Urban settlement monitoring based on PS-InSAR

The PS-InSAR method is mainly used in urban deformation monitoring. The processing flow is as follows : Firstly, based on the principle of three baselines and minimum baseline, the main image is selected, and the auxiliary image is registered and resampled in turn. Then, after the interference processing of the main and secondary images, the differential interference atlas is generated by combining the DEM data, and the PS points are selected by the Amplitude Dispersion Index (ADI) method. The Delaunay triangulation algorithm of PS is established again to separate the nonlinear deformation, Atmosphere Phase Screen (APS) and noise in the residual phase. The overall range of APS is estimated by using Kriging difference, and PS points are selected again. The multi-image sparse grid phase unwrapping is performed again, and finally the final deformation estimation of each PS point is obtained.
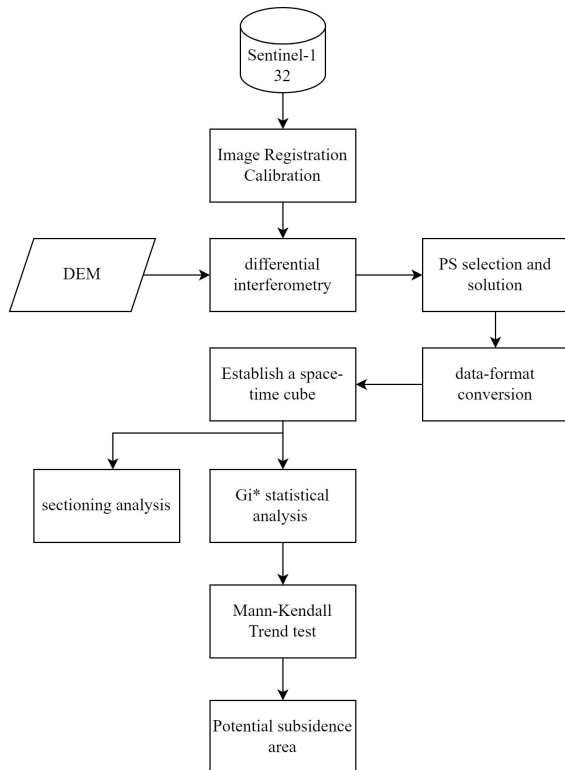
ID	Name	Value
1	Coordinate system	CGCS2000
2	Time step interval	12 D
3	Aggregate shape type	FISHNET_GRID
4	Distance interval	100 M
5	Summary field	VALUE
6	Statistical value	MEAN-Calculates
7	Filling Cube Graphs	SPACE_TIME_NEIGHBORS

Table 1. Parameter of space-time cube

The spatio-temporal hotspot analysis algorithm is shown in Figure 2c. Firstly, the spatio-temporal Getis-Ord Gi * statistics(Sukmaniar et al., 2020) (as Equations 1) are performed on each bin to obtain the z-score value of each bin, that is, the continuous deformation value in the cumulative deformation period is obtained. Then, based on this value, the K nearest neighbor clustering algorithm is used in the space-time domain to obtain the deformation hot and cold spots in the demonstration area. Mann-Kendall(Hamed and Ramachandra Rao, 1998) (as Equations 2, 3) was used again to evaluate the trend test of cold spots and hot spots of deformation, and finally the overall trend change of deformation in time and space domain was obtained.
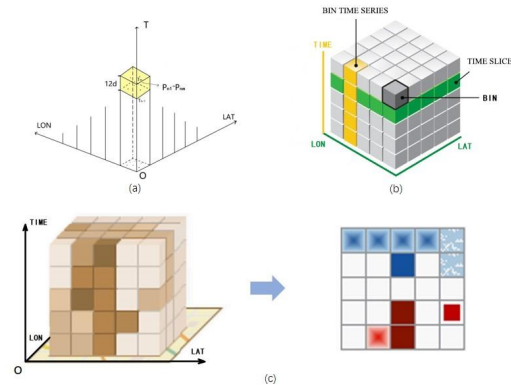

Figure 1. The algorithm flow

Figure 2. Illustration of space-time cube (ESRI, 2022)

2.3 Emerging Spatial and Temporal Hotspot Analysis Methodology

Since the settlement data is a point-like vector format, first of all, it is necessary to do relevant preprocessing and convert it into a space-time cube format. The specific conversion parameters are shown in Table 1, where the time domain sampling of the cube is set to 12 days, and the spatial domain sampling is set to 100 * 100m. The average value is filled, and the true meaning of each cube bin (as shown in Figure 2b) is the average deformationin(Prasannakumar et al., 2011) the range of 100 * 100m and 12 days.

$$G_i^* = \frac{\sum_{j=1}^{n} w_{i,j} x_j - \overline{X} \sum_{j=1}^{n} w_{i,j}}{S \sqrt{\frac{\left[n \sum_{j=1}^{n} w_{i,j}^2 - \left(\sum_{j=1}^{n} w_{i,j} \right)^2 \right]}{n-1}}}, \qquad (1)$$

where x_j is the value of bin; w_{ij} is the spatial weight of elements i and j, n is the total number of elements.

$$\overline{X} = \frac{\sum_{j=1}^{n} x_j}{n}, \qquad S = \sqrt{\frac{\sum_{j=1}^{n} x_j^2}{n} - \left(\overline{X} \right)^2}$$

$$S = \sum_{i=1}^{n-1} \sum_{j=i+1}^{n} \operatorname{sgn}\left(x_j - x_i \right), \qquad (2)$$

$$VAR(S) = \frac{n(n-1)(2n+5) - \sum_{k=1}^{p} q_k(q_k-1)(2q_k+5)}{18}, \qquad (3)$$

where p is the number of equivalent groups in the bin value, and qk is the number of bin values in the kth group. By using the Equations (4), the S is transformed into the test statistic

ZMK.When the sample size is large, ZMK can approximately meet the standard normal distribution, ZMK > 0 indicates that the deformationin has an increasing trend, and ZMK < 0 indicates that the deformationin has a downward trend.

$$Z_{MK} = \begin{cases} \dfrac{S-1}{VAR(S)} & ; \quad S > 0 \\[2mm] 0 & ; \quad S = 0 \\[2mm] \dfrac{S+1}{VAR(S)} & ; \quad S < 0 \end{cases}, \quad (4)$$

3. Study Area And Data

3.1 Study area

Beijing is located at 115.7° to 117.4° E, 39.4° to 41.6° N, with a total area of 16410.5 km². As shown in Figure 3, from northwest to southeast, the orderly arrangement of mountains, hills, hillocks and alluvial plains is presented. Due to the large amount of groundwater exploitation, a number of subsidence funnel diffusion areas have been formed(Yang et al., 2012). At present, the subsidence area from Chaoyang to Tongzhou is connected into one area, which has become the most developed area in Beijing plain. As the sub-center of Beijing, Tongzhou District has a large number of new buildings and road networks, and the population and industries are growing rapidly. According to the existing research conclusions, there is a large amount of settlement around the sub-center of Beijing, and it is the main settlement area.
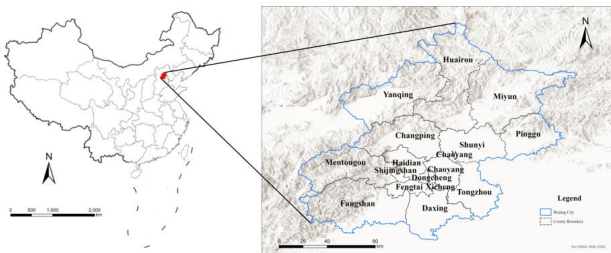

Figure 3. Overview of The Study Area

3.2 Data sources

In this paper, the C-band Sentinel-1B Interferometric Wide Swath (IW) model data from November 2016 to January 2018 are selected. The spatial range is shown in Figure 4, covering a total of 32 scenes including western Tianjin, northern Hebei and main urban areas of Beijing. The Sentinel-1B data(Torres et al., 2012) is detailed in Table 2. This paper chooses the VV polarization method as the main experimental data.

4. Experiment and Result

4.1 Settlement monitoring results

Using the PS-InSAR method, 292,309 permanent scatterer monitoring points were obtained, and the Line of Sight (LOS) subsidence in Beijing from 2016 to 2018 was further obtained, and the deformation of LOS direction was converted into vertical deformation, as shown in Figure 5. Figure 5a shows that Fengtai, Mentougou, Shijingshan, Dongcheng and Xicheng in the central and western parts of Beijing are in a stable state during the monitoring period, and there is no large-scale settlement. However, an obvious inverted triangular settlement development zone is formed at the junction of Chaoyang and

Tongzhou in the east. The cumulative settlement during the study period is from -49 to -135mm. The settlement of the eastern boundary of Chaoyang District in Figure 5 (c) is the most serious, and there are multiple local high-value (from -103 to -135mm) settlement areas.
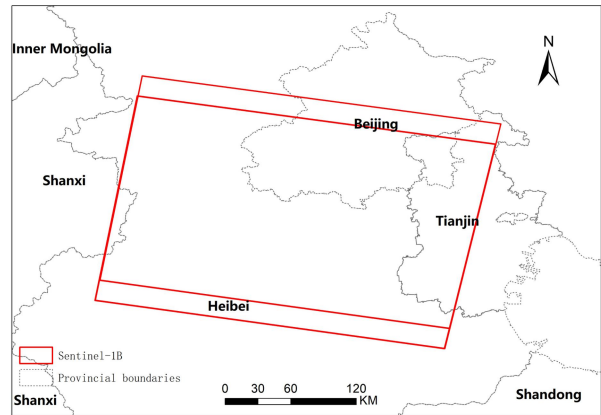

Figure 4. Sentinel-1B data range

ID	Name	Parameter
1	Orbit type	Near Polar Sunsynchronous Orbit
2	Orbital altitude	693 km
3	Design life	7.25 years
4	Band / Wavelength / Frequency	C-band / 5.55cm / 5.405GHz
5	Return period	12 days for single star 6 days for double stars
6	Side view direction	Right View
7	IW Model Spatial resolution width	Polarization Mode: VH+VV Range:5m, Azimuth:20m 250 km

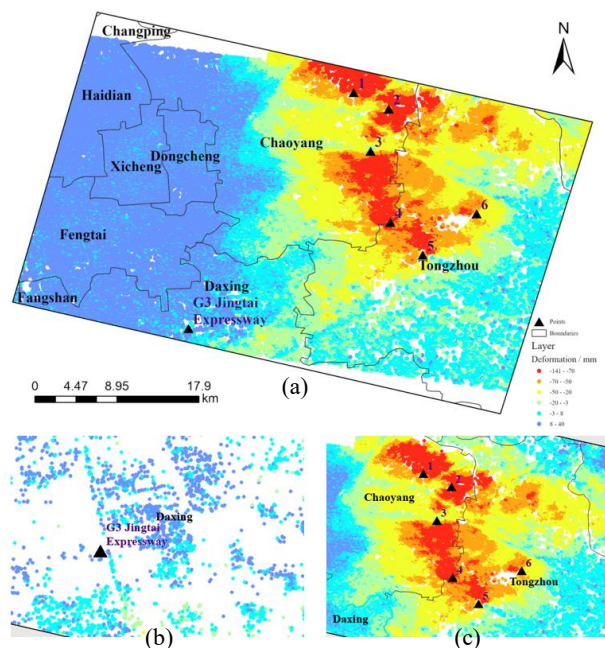Table 2. Sentinel-1B detailed parameters

Figure 5. Cumulative settlement map from 2016 to 2018

Figure 6a shows the statistics of the settlement rate distribution. It can be seen that it obeys the normal distribution with a mean of 0 and has a peak at -10mm / a, indicating that the settlement rate in the settlement area is concentrated at about 10 ± 5mm / a, and the surface deformation area of Beijing is larger. The settlement results are displayed in a three-dimensional form, where the Z axis represents the cumulative deformation variable. Slice1 (116.455°, 39.593°), Slice2 (116.525°, 39.584°), and Slice3 (116.588°, 39.575°) are sliced and analyzed, and their section statistics are counted. The results are shown in Figure 6b, indicating that there is a spatial correlation between the cumulative settlement and the settlement rate, which cannot be reflected by the conventional method, and the clustering geospatial analysis cannot be accurately performed from the time dimension. It also cannot reflect the development and change of deformation in the time dimension, so a new space-time analysis theory strategy is needed.
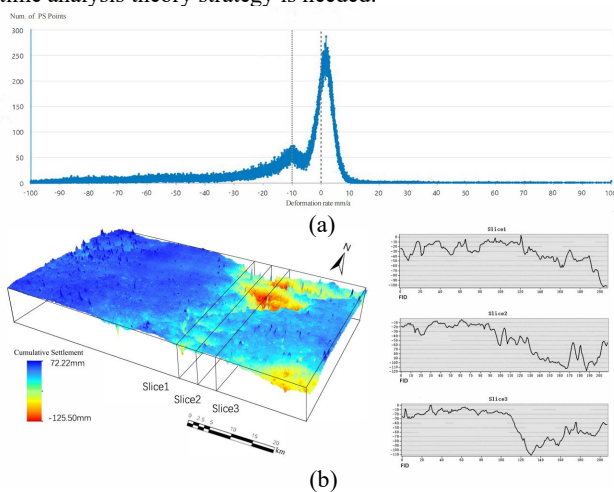

(a)

(b)

Figure 6. Accumulative deformation statistics and sectional drawing

4.2 Analysis of urban deformation based on space-time cube

Based on the deformation results of PS-InSAR, through coordinate transformation, format conversion and other preprocessing work, a three-dimensional display of space-time cube is created as shown in Figure 7. The main difference from Figure 6 is that the Z-axis is the time dimension, while the real deformation bin value is the fourth dimension, which is usually displayed by color strips. The same geographical location (SliceA, SliceB, SliceC) in Figure 6 is selected to analyze the section of the space-time cube (as shown in Figure 7), indicating that the settlement changes with time, especially in urban areas. The two slices of Slice1 (Figure 7) and SliceA (Figure 6) are selected for horizontal comparison, which shows that the two are the same in the overall deformation trend, but Slice A can reflect the development trend of settlement value in time series, and can obtain more information than Slice1. As shown in Figure 7, the three points of Sa1, Sa2 and Sa3 in Slice A are not continuous in time series and the initial settlement time is also different, indicating that the three surface subsidences have been uplifted in the later period and offset the original subsidence. The causes of deformation and geological stress are more complex and need further study.

4.3 Emerging spatio-temporal hotspots (ESH) analysis

ESH analysis can solve the trend discrimination of Bin value in time dimension in space-time cube. The trends obtained by

analysis are divided into 17 categories, including new, continuous, strengthening, continuous, decreasing, scattered, oscillating, and historical hot and cold spots. A total of 10 trends were detected in this experiment. The Trend Z-Score and Trend P-Value of each trend class are shown in Table 3.
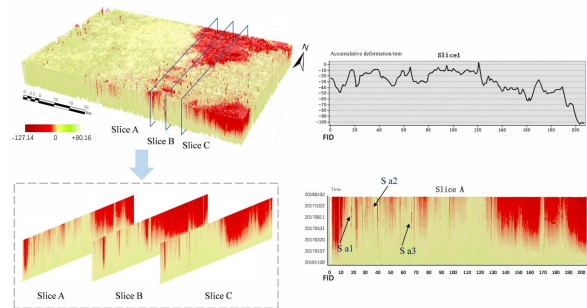

Figure 7. The analyse result of space-time cube Slice

Pattern Type	Trend Z-Score	Trend P-Value	Max Percent Significant Cold Spot
Intensifying Hot Spot	1.647366≤	0.099483≥	0
Consecutive Hot Spot	3.607164≤	0.00031≥	0
Persistent Hot Spot	-1.619127≤	1≥	0
Sporadic Hot Spot	-5.25453≤	1≥	0
Diminishing Hot Spot	-5.197724≤	0.099483≥	0
Historical Hot Spot	-4.998904≤	0.977341≥	0
Oscillating Cold Spot	5.714286≤	2.385841≥	82.857143
New Cold Spot	-8.236831≤	0.754713≥	2.857143
Sporadic Cold Spot	-8.322039≤	0.267986≥	68.571429
Consecutive Cold Spot	-8.435651≤	0.021412≥	88.571429

Table 3. Trend Z-Score and Trend P-Value by Trend Category

The ESH analysis based on the settlement results of Beijing is shown in Figure 8. The cold spots and hot spots are distributed in the east and west parts respectively, and the meaning of the cold spot is the Part of the surface subsidence. Six main trend results were detected, such as Oscillating Cold Spot, Consecutive Cold Spot, No Pattern Detected, and New Cold Spot, accounting for 31%, 18%, 17%, 31%, and 1%, respectively. This paper only focuses on the distribution of cold spots. The result shows that the trend of cold spots is highly consistent with the settlement area of Figure 7. The junction of Tongzhou District and Chaoyang District is detected as a continuous cold spot in EHS analysis, and is surrounded by oscillating cold spots, forming a settlement range with oscillating cold spots as a buffer zone.

There are three main trends of consecutive cold point, oscillating cold point and new cold point, as shown in Figure 9, and we select some typical points from them in the real remote sensing image display as shown in Figure 10. Figure 9(a) shows the consecutive distribution range and characteristic trend of cold spots. From the perspective of spatial dimension, there are multiple subsidence centers in the study area. The largest subsidence area is centered on the Bali Bridge of the subway

and forms an ellipse along the Batong district of Line 1, and other subsidence areas extend in a decentralized form to the north and south. The characteristic trend diagram is a curve with a stable negative slope, indicating that the area continues to settle and is less affected by the season. In Figure 9b, the distribution of the oscillating cold spots is in the characteristic trend map, and it is found that the range of the oscillating cold spots diffuses away with the boundary of the continuous cold spots, forming a large buffer zone. In addition, there are more

local oscillating subsidence areas in Daxing and southern Tongzhou. The overall trend characteristic map is in the settlement trend, but the broken line fluctuates more, and the standard deviation expectation (Mean STD) of the settlement value is 30.263 mm, indicating that the region is greatly affected by season and precipitation in the process of surface settlement. Figure 9c shows the distribution of new cold spots. It can be observed that the new cold spots are distributed along the outer edge (as shown in Figure 10) of the oscillating cold spots.
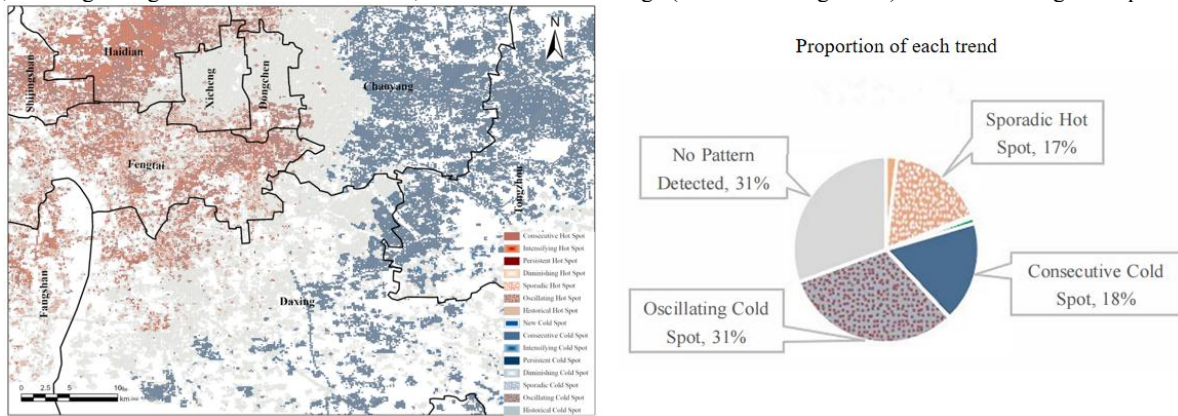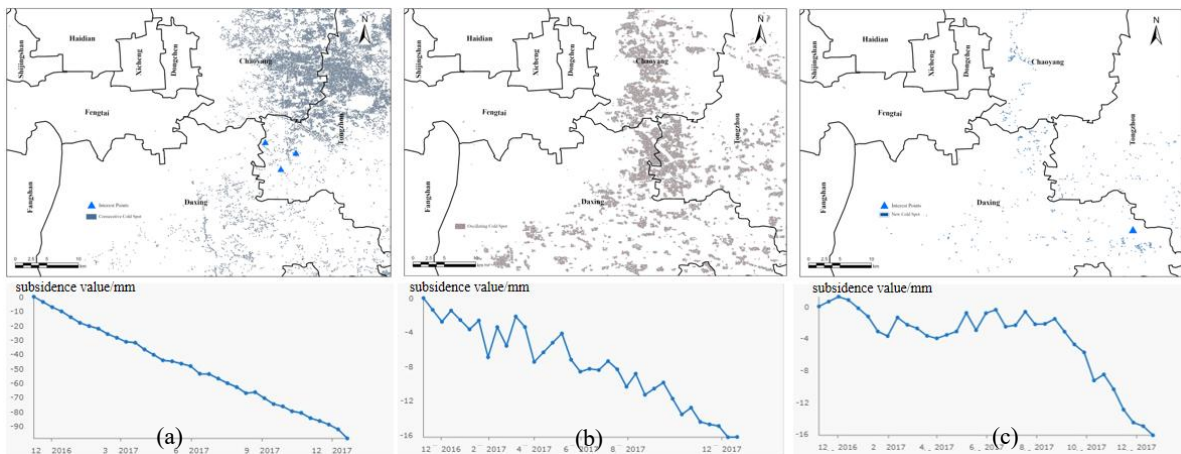

Figure 8. Emerging Hot Spot Analysis of Beijing

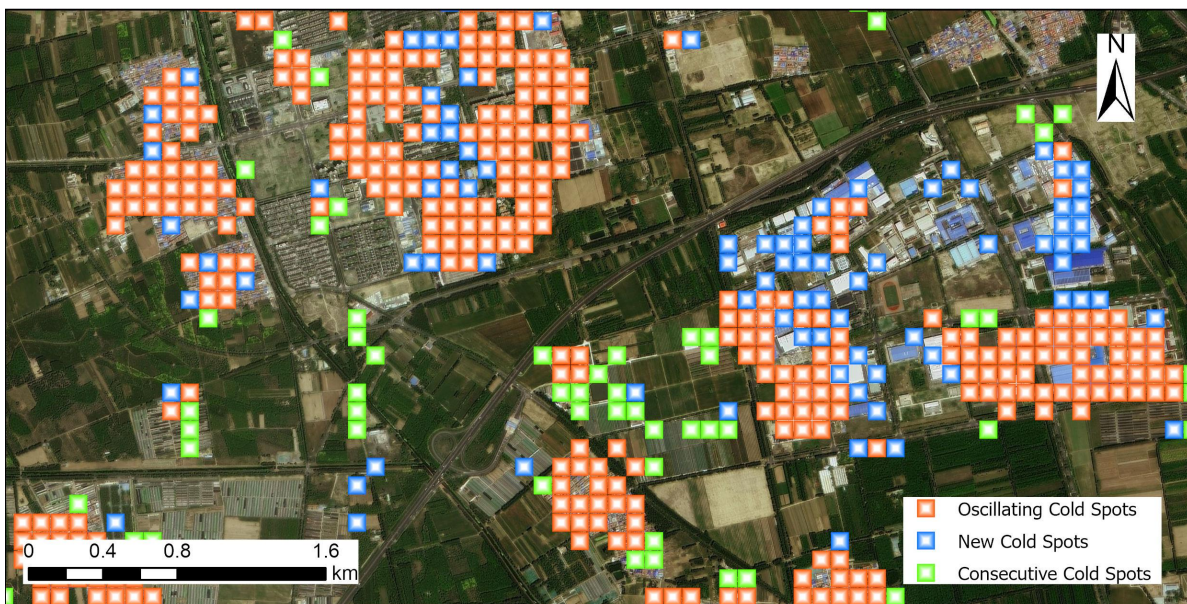Figure 9. Cold Spot Distribution Map

Figure 10. The actual distribution of emerging spatio-temporal hotspots

5. Conclusion

In this paper, a space-time cube is constructed for the settlement phenomenon in Beijing. Different from the previous methods of settlement analysis and display, the space-time cube is more intuitive and easy to understand. It is convenient to view the spatial and temporal distribution of high-value settlement through attribute filtering. Based on the space-time cube, a new space-time analysis method is proposed to directly analyze the law of settlement development. Firstly, the data is reorganized to construct a spatio-temporal cube at a certain spatial and temporal interval. On this basis, the K-nearest neighbor spatial relationship is used to select the spatio-temporal analysis range. Secondly, ESH analysis, Getis-Ord Gi* statistics and Mann-Kendall test were used to analyze the settlement trend of space-time cube. Finally, the study was divided into 10 kinds of settlement trends, and the continuous cold spots and oscillating cold spots in the settlement area were obtained. It is found that the junction of the eastern part of Chaoyang and the western part of Tongzhou is a continuous settlement area, which coincides with the center of the settlement funnel, and is surrounded by the oscillating settlement area to form a settlement buffer zone. In addition, a number of continuous subsidence areas were also found in the oscillating subsidence area, which were very likely to become potential subsidence centers, which could not be detected by ordinary analysis. The analysis method of space-time synergy combined with trend test provides a new idea for the trend analysis of urban settlement, and also provides data for urban settlement safety warning to take appropriate preventive measures.

In view of the fact that settlement is affected by many factors, there is a certain complexity and error in the modeling and analysis of architecture, geology and hydrology in the study area. In this paper, a new spatio-temporal analysis method based on statistical analysis is used to directly explore the regional subsidence model. However, there are some problems in the emerging space-time analysis method based on settlement. For example, the size of fishing grid setting is too small, which leads to too many space-time cubes and long data processing time. The grid setting is too large to cause the analysis accuracy to decrease; because the settlement process is slow, the development time of settlement is different under different geological conditions, so it is necessary to select the appropriate analysis time step. Considering the spatial correlation between the PS point selection mask of the settlement data and the spatial correlation of the settlement, the selected spatial relationship must not only ensure that there is enough space-time cube analysis, but also ensure that the model is in line with the actual situation. Incorrect spatial relationship selection will lead to abnormal p-Value and z-Score, resulting in wrong settlement trend. Therefore, in further research, a specific time analysis range should be set for different analysis grids in combination with geology, and a variety of spatial relationship fusion analysis methods should be explored according to different data conditions to ensure the accuracy of model analysis and results.

Acknowledgements

.

References

Cigna, F. and Tapete, D., 2022. Urban growth and land subsidence: Multi-decadal investigation using human settlement data and satellite InSAR in Morelia, Mexico. *Science of The Total Environment*, 811: 152211.

Crosetto, M., Monserrat, O., Cuevas-González, M., Devanthéry, N. and Crippa, B., 2016. Persistent Scatterer Interferometry: A review. *ISPRS Journal of Photogrammetry and Remote Sensing,* 115: 78-89.

ESRI, 2022. Create Space Time Cube By Aggregating Points *ArcGIS Pro Usage Manual.*

Ferretti, A., Prati, C. and Rocca, F., 2001. Permanent scatterers in SAR interferometry. *IEEE Transactions on Geoscience and Remote Sensing*, 39(1): 8-20.

Foroughnia, F., Nemati, S., Maghsoudi, Y. and Perissin, D., 2019. An iterative PS-InSAR method for the analysis of large spatio-temporal baseline data stacks for land subsidence estimation. *INTERNATIONAL JOURNAL OF APPLIED EARTH OBSERVATION AND GEOINFORMATION,* 74: 248-258.

Hamed, K.H. and Ramachandra Rao, A., 1998. A modified Mann-Kendall trend test for autocorrelated data. *Journal of Hydrology*, 204(1): 182-196.

He, X. et al., 2022. Spatio-Temporal Analysis of Land Subsidence in Beijing Plain Based on InSAR and PCA. *Spectroscopy and Spectral Analysis*, 42(07): 2315-2324.

Prasannakumar, V., Vijith, H., Charutha, R. and Geetha, N., 2011. Spatio-Temporal Clustering of Road Accidents: GIS Based Analysis and Assessment. *Procedia - Social and Behavioral Sciences*, 21: 317-325.

Ramirez, R.A.A. et al., 2022. Monitoring of construction-induced urban ground deformations using Sentinel-1 PS-InSAR: The case study of tunneling in Dangjin, Korea. *INTERNATIONAL JOURNAL OF APPLIED EARTH OBSERVATION AND GEOINFORMATION*, 108.

Sukmaniar, S., Kurniawan, A. and Pitoyo, A., 2020. Population characteristics and distribution patterns of slum areas in Palembang City: Getis ord Gi* analysis. *E3S Web of Conferences*, 200: 04005.

Torres, R. et al., 2012. GMES Sentinel-1 mission. *REMOTE SENSING OF ENVIRONMENT*, 120: 9-24.

Yang, Y. et al., 2012. Influence of South to North Water Transfer on groundwater dynamic change in Beijing plain. *Environmental Earth Sciences*, 65(4): 1323-1331.

Yang, Y., Wang, R., Zhou, Y., Jiang, Y. and Wang, X., 2015. The interaction between land subsidence and urban development in China, *International Symposium on Land Subsidence*.